Spatial synchrony in sub-arctic geometrid moth outbreaks reflects dispersal in larval and adult lifecycle stages

Ole Petter Laksforsmo Vindstad[1]* (ole.p.vindstad@uit.no), Jane Uhd Jepsen[2] (jane.jepsen@nina.no), Nigel Gilles Yoccoz[1] (nigel.yoccoz@uit.no), Ottar N. Bjørnstad[3] (onb1@psu.edu), Michel d. S. Mesquita[4, 5] (mmeclimate@gmail.com) & Rolf Anker Ims[1] (rolf.ims@uit.no)

[1] Department of Arctic and Marine Biology, University of Tromsø – The Arctic University of Norway, Framstredet 39, N-9037 Tromsø, Norway

[2] Norwegian Institute for Nature Research, Fram Centre, N-9296 Tromsø, Norway

[3] Department of Biology, Pennsylvania State University, 515 ASI Building, University Park, PA 16802

[4] Future Solutions, Håvikbrekka 92, 5440 Mosterhamn, Norway

[5] Uni Research Climate, Bjerknes Centre for Climate Research, Jahnebakken 5, Bergen 5007, Norway

* Correspondence author: Ole Petter Laksforsmo Vindstad. Department of Arctic and Marine Biology, University of Tromsø – The Arctic University of Norway, Framstredet 39, N-9037 Tromsø, Norway. Phone: (+47) 99791636. E-mail: ole.p.vindstad@uit.no

Running title: Geometrid spatial synchrony

Keywords (max 8): *Epirrita autumnata*, *Operophtera brumata*, wind-driven dispersal, ballooning, dispersal barrier, inter-species comparison, population cycle, travelling wave

Statement of authorship: RAI and NGY conceived and designed the study. OPLV, RAI and JUJ collected the data. OPLV and ONB analyzed the data with contributions from JUJ, NGY and RAI. OPLV wrote the paper with input from all co-authors. All authors contributed to manuscript editing.

Abstract

1. Spatial synchrony in population dynamics can be caused by dispersal or spatially correlated variation in environmental factors like weather (Moran effect). Distinguishing between these mechanisms is challenging for natural populations, and the study of dispersal-induced synchrony in particular has been dominated by theoretical modelling and laboratory experiments.

2. The goal of the present study was to evaluate the evidence for dispersal as a cause of meso-scale (distances of tens of kilometers) spatial synchrony in natural populations of the two cyclic geometrid moths *Epirrita autumnata* and *Operophtera brumata* in sub-arctic mountain birch forest in northern Norway.

3. To infer the role of dispersal in geometrid synchrony, we applied three complementary approaches, namely estimating the effect of design-based dispersal barriers (open sea) on synchrony, comparing the strength of synchrony between *E. autumnata* (winged adults) and the less dispersive *O. brumata* (wingless adult females), and relating the directionality (anisotropy) of synchrony to the predominant wind directions during spring, when geometrid larvae engage in windborne dispersal (ballooning).

4. The estimated effect of dispersal barriers on synchrony was almost three times stronger for the less dispersive *O. brumata* than *E. autumnata*. Inter-site synchrony was also weakest for *O. brumata* at all spatial lags. Both observations argue for adult dispersal as an important synchronizing mechanism at the spatial scales considered. Further, synchrony in both moth species showed distinct anisotropy and was most spatially extensive parallel to the east-west axis, coinciding closely with the overall dominant wind direction. This argues for a synchronizing effect of windborne larval dispersal. Congruent with most extensive dispersal along the east-west axis, *E. autumnata* also showed evidence for a travelling wave moving southwards at a speed of 50-80 km/year.

5. Our results suggest that dispersal processes can leave clear signatures in both the strength and directionality of synchrony in field populations, and highlight wind-driven dispersal as promising avenue for further research on spatial synchrony in natural insect populations.

Introduction

Spatial synchrony in population dynamics has been documented in a wide range of taxa (Peltonen *et al.* 2002; Liebhold, Koenig & Bjørnstad 2004; Haynes *et al.* 2013; Gouveia, Bjørnstad & Tkadlec 2016).

Although spatial synchrony is a common phenomenon, the underlying mechanisms are rarely well-documented. Generally, synchrony can have three mutually non-exclusive causes: 1) Dispersal of the focal species between populations, 2) dispersal of natural enemies of the focal species and 3) spatially correlated environmental variation that affects population dynamics, e.g. weather patterns or extreme events (i.e. the Moran effect). However, most field studies of synchrony have been limited to describing the spatial scale and variation of synchrony, and relatively few have been able to link the observed patterns of synchrony to the underlying mechanisms [see Grenfell *et al.* (1998), Ims & Andreassen (2000), Post & Forchhammer (2002), Ims & Andreassen (2005) and Roland & Matter (2007)].

An obstacle to disentangling the roles of dispersal and Moran effect is the fact that the rate and scale of dispersal is difficult to observe and quantify directly for most organisms. However, carefully designed studies may provide several indirect lines of evidence for dispersal as a synchronizing mechanism (Bjørnstad, Ims & Lambin 1999). First, expected dispersal barriers may be strategically incorporated into the spatial sampling frame of studies (Ims *et al.* 2004). A clear drop in synchrony across a dispersal barrier argues for a synchronizing effect of dispersal. Conversely, if synchrony is unaffected by dispersal barriers, the Moran effect is likely to be operating (Grenfell *et al.* 1998). Targeted sampling designs of this type are extremely rare, however. Indeed, most studies of synchrony are based on time series that have been sampled for other purposes. Second, if processes that are linked to dispersal can be related to synchrony, a synchronizing effect of dispersal may be inferred (Anderson *et al.* 2018). For example, dispersal in many insect species is aided by wind (Straussfogel *et al.* 2008). Hence, if spatial patterns of synchrony can be linked to wind patterns, windborne dispersal is a likely synchronizing mechanism (Bearup *et al.* 2013). Finally, the extent of synchrony may be compared between species that differ in dispersal capacity, but are expected to show similar responses to environmental factors. Everything else being equal, a more dispersive species should display higher levels of spatial synchrony if dispersal is an important synchronizing mechanism (Koenig 1998; Paradis *et al.* 1999; Chevalier, Laffaille & Grenouillet 2014).

In the present study, we implement all of these approaches for a pair of sympatric geometrid (Lepidoptera: Geometridae) moths – *Epirrita autumnata* Bkh. (autumnal moth) and *Operophtera brumata* L. (winter moth) – inhabiting the mountain birch (*Betula pubescens* var. *pumila* Orlova) forest of northern Fennoscandia. The system is a classic example of population cycles, with both moth species showing fairly regular 9-10-year population cycles (Tenow 1972; Myers & Cory 2013). There is ample evidence that climatically induced Moran effects produce spatial synchrony in moth populations across distances of hundreds of kilometers (Klemola, Huitu & Ruohomaki 2006; Jepsen *et al.* 2009). Meanwhile, the contribution of dispersal to spatial synchrony in the system is unclear. Early instar moth larvae disperse by wind with the aid of silken threads – so-called "ballooning". Ballooning has traditionally been assumed to carry the larvae a few hundred meters at most (Edland 1971), but more recent genetic evidence suggests that the mechanism may operate across distances of tens of kilometers (Leggett *et al.* 2011). The dispersal capacity of adult moths of these species is poorly known, but males of both *E. autumnata* and *O. brumata,* and females *of E. autumnata,* have well-developed wings, and can probably disperse over many kilometers. Based on genetic data, Snäll *et al*. (2004) concluded that substantial dispersal over distances of at least 19 km was likely for *E. autumnata*, although without being able to distinguish between the effects of larval and adult dispersal. Meanwhile, females of *O. brumata* are wingless, and thus expected to disperse over distances of only a few meters. Moreover, the wingspan of *E. autumnata* generally exceeds that of male *O. brumata*, leading to the expectation of higher dispersal capacity in the former species (Sandhya 2012). Based on these biological traits, we might expect that the dispersal capacity of the two moth species is similar during the larval stage, but lower for *O. brumata* than *E. autumnata* during the adult stage.

In accordance with differential adult dispersal capacity in the two moth species, Hagen *et al.* (2008) found lower levels of spatial synchrony for *O. brumata* than *E. autumnata* at very local scales (<600m), arguing for adult dispersal as an important synchronizing mechanism locally. Meanwhile, Ims *et al.* (2004) reported spatial asynchrony between *O. brumata* populations separated by distances of 4-9 km, suggesting that both dispersal and the Moran effect have limited impacts on the meso-scale spatial dynamics of *O. brumata* in the mountain birch system. However, the latter study was based on a time

112 series of only four years, and data for *E. autumnata* was not presented for comparison with *O. brumata*.
113 Over a decade later, a more comprehensive assessment of meso-scale patterns of spatial synchrony, and
114 their relationship with dispersal, is still lacking for these otherwise well-studied geometrids.
115
116 Another point of contention regarding the spatial dynamics of geometrid moths is the phenomenon of
117 travelling waves (Sherratt & Smith 2008). The possibility that geometrid outbreaks travel as waves
118 across distances of thousands of kilometers has been advocated based on qualitative time series of
119 outbreak records (Tenow *et al.* 2013), but the validity of this claim has been questioned on both
120 conceptual and analytical grounds (Jepsen *et al.* 2016; Tenow 2016). Meanwhile, there is a conspicuous
121 absence of studies that employ quantitative population data to evaluate the presence of geometrid waves
122 on more modest scales, where the existence of waves would be easier to reconcile both with general
123 theory (Sherratt & Smith 2008) and empirical experience from other systems (Moss, Elston & Watson
124 2000; Bjørnstad *et al.* 2002; Berthier *et al.* 2014).
125
126 In the present paper, we address the outlined knowledge gaps by means of 19-year datasets for both *O.*
127 *brumata* and *E. autumnata*, derived from the design that was used by Ims *et al.* (2004). The setting for
128 the study is the coastal region of Troms County in northern Norway. This area has a complex
129 topography, with numerous fjords, mountains and islands. Patches of mountain birch forest occur
130 throughout the region, wherever conditions are suitable, and these make perfect habitat for moth
131 populations. Our design takes advantage of this naturally fragmented habitat to introduce dispersal
132 barriers into the sampling frame. Specifically, our setup consists of 120 sampling sites, organized into
133 12 transects which are spread out across the study region. The transects are grouped into six pairs, with
134 an expected dispersal barrier in the form of a stretch of open sea or alpine terrain located between the
135 two transects within each pair (Fig. 1). Based on this unique design, we evaluate the evidence for
136 dispersal as a driver of meso-scale spatial synchrony in the focal geometrids. First, to test whether adult
137 dispersal contributes to synchrony, we compare the drop in synchrony across dispersal barriers and
138 across the whole study region between *E. autumnata* (winged females) and *O. brumata* (wingless
139 females). Second, to test whether wind-driven larval dispersal contributes to synchrony, we determine

the directionality (anisotropy) of synchrony and compare this to the predominant wind direction across the study region during the period of larval dispersal. Finally, we study the time-lagged directionality of synchrony to look for evidence of travelling waves.

Materials and methods

Study system

Our study region in North-west Norway (69°30′ to 70°03′N; 18° to 20°E) is characterized by an oceanic, sub-arctic climate, with cool summers (average temperature in July in the range of 12 to 13 °C) and mild winters (average temperature in January in the range of -2 to -5 °C). The forest of the region is dominated by mountain birch, with sporadic occurrences of aspen (*Populus tremula* L.), rowan (*Sorbus aucuparia* L.) and planted spruce (*Picea abies* L.). Owing to the mountainous topography of the region, mountain birch forest usually occurs as narrow belts between the sea and the alpine tree line (250-300 m. a. s. l.). *E. autumnata* and *O. brumata* are the most abundant insect herbivores in the system (Bylund 1999), and have very similar univoltine lifecycles. Moth larvae hatch from overwintering eggs around the time of birch budburst and start feeding on young birch leaves. Budburst usually occurs in mid-May, but can vary by as much as three weeks between years (Karlsen *et al.* 2007). Windborne dispersal of ballooning larvae takes place during the early stages of larval development, occurring throughout May and early June depending on spring phenology. Newly hatched larvae of *E. autumnata* are slightly larger and heavier than those of *O. brumata* (personal observation by the authors), but the impact of this difference on the capacity for ballooning is currently unknown. The larval stage includes five instars, and usually lasts until early to mid-July, when the larvae pupate in the ground. Adults of *E. autumnata* emerge in August-September, while *O. brumata* adults emerge in September-October. The adult moths lay their eggs on the trunks and branches of birch trees.

Study design

Our design consists of a spatial panel of sampling sites, spread out across an area of approximately 50 × 80 km (Fig. 1). The design encompasses twelve main locations, each harboring an approximately 1.8 km long transect, running through a continuous stretch of mature mountain birch forest. Within each

transect, there are 10 permanent sampling sites, separated by about 200 m. The mean transect-level elevation ranges between 43 and 176 m. a. s. l. (transect 11 and 3, respectively), but most transects have an elevation of around 100 m. The twelve transects are arranged into six pairs. Within each pair, one transect is located on a very large island or the mainland (hereafter "continental" transects) and the other is located on a medium-sized island (hereafter "island" transects). Transect 3 is defined as an island transect although it is not located on an island in the strict sense, but in a stand of birch forest in a valley that is surrounded by mountains. The straight-line distance (hereafter 'distance') between transects within pairs is between 4.48 and 8.59 km (mean 5.65 km). This distance always includes a stretch of open sea (or alpine tundra for transect 3) of at least 1.5 km. Given the quite limited dispersal distances reported in the only study of geometrid ballooning known to us (Edland 1971), we expected these stretches of non-habitat to constitute a substantial dispersal barrier for moth larvae.

Every summer since 1999, we have estimated the density of moth larvae at all sampling sites. To do this, we gathered ten birch branches of about 80 cm length from haphazardly chosen birch trees within a 20 m radius around each site. The branches were thoroughly shaken in a large plastic box, until all moth larvae had detached and fallen into the box. The larvae were subsequently sorted to species and counted. To ensure that the larvae were large enough to be easily observed, we timed the density measurements to the later instars of the larval stage, usually occurring in late June to early July. This implies that most *E. autumnata* larvae were in the 5^{th} instar when they were counted, while most *O. brumata* larvae (whose phenology is somewhat delayed relative to *E. autumnata*) were in the 4^{th} instar. Since the two moth species feed sympatrically on mountain birch, this method allowed us to obtain parallel time series of both.

For studying the relationship between spatial synchrony and wind, we defined the period of potential windborne larval dispersal as May 1 to June 15. According to the experience of the authors, this covers the entire period when early-instar larvae, which are capable of ballooning, can potentially be found in the coastal mountain birch forests, taking into account phenological variation introduced both by between-year variation in weather and spatial climatic gradients (Mjaaseth *et al.* 2005). The wind data

196 used were the daily ERA Interim reanalysis [for a closer description, see Mesquita *et al.* (2015) and
197 references therein, such as Dee *et al.* (2011)]. The data were downloaded from
198 http://apps.ecmwf.int/datasets/data/interim-full-daily/levtype=sfc/, and interpolated to 12.5 x 12.5 km.
199 We extracted average wind directions and average wind speeds every 6 hours for a box of 50 × 80 km
200 (69°25' to 70°15' N and 17°45' to 20°55' E), covering all of the samplings sites in the design. The
201 program CDO (Climate Data Operators, Max-Planck Institute,) was used to extract the box and calculate
202 the averages. Since very weak winds would be unlikely to carry the larvae beyond the local scale, we
203 subsetted the wind data to include only winds with a speed of more than 6 m/s (light breeze) before
204 further analysis. Furthermore, because the dispersal patterns of adult *E. autumnata* might also affected
205 by wind, we extracted wind data according to the same procedure for the period of potential adult
206 dispersal of this species during autumn. This period was defined as August 1 to September 15.
207
208 *Statistical analyzes*
209 We used the correlation in population growth rates [$r_t = \log_e(N_t/N_{t-1})$, where N is larval density, and a
210 constant of 1 was added to N to avoid zero entries] between sites as a measure of the strength of
211 synchrony between them. All analyzes were based on site-level correlations and were conducted
212 separately for *E. autumnata* and *O. brumata*. The analyzes were conducted with R version 3.4.0 (R
213 Developement Core Team 2017) using libraries and functions detailed below. All average directions
214 were calculated using circular statistics (Jammalamadaka & Sengupta 2001).
215
216 The first step of the analysis was to characterize the overall relationship between synchrony and inter-
217 site distance across the study region. To do this, we used the `Sncf` function in the `ncf` library to fit
218 nonparametric non-directional (isotropic) correlation functions to the matrix of cross-correlations
219 between all pairs of sites (Bjørnstad & Falck 2001). To reduce the impact of random noise and focus on
220 the overall regional patterns of synchrony, we estimated the functions using splines with 6 degrees-of-
221 freedom. This was also done for the analysis of directional synchrony below. Subsequently, we focused
222 on estimating the drop in synchrony across our design-based dispersal barrier, i.e. open sea within island-
223 continent pairs. To do this, we used linear mixed models with the between-site correlations within pairs

as the response variable. The distinction between correlations within transects and between transects (i.e. across sea) was taken as a two-level fixed predictor variable. Hence, the models estimated the drop in correlation when moving across sea, using the within-transect correlation as a reference point. The model included random slopes and intercepts for each island-continent pair, to account for variation in the strength of synchrony between pairs. Further, to provide an assessment of how the drop in synchrony across sea compared to the drop in synchrony with distance within core birch forest habitat, we fitted a linear mixed model taking the correlations within transects as the response and distance as the predictor. Applying a linear model was considered parsimonious, as nonparametric functions fitted during exploratory analyzes produced linear relationships between synchrony and distance within most transects. Random slopes and intercepts were modelled for each transect, to account for variability in the linear synchrony-distance relationship. The fitted model was then used to extrapolate the synchrony-distance relationship observed within transects to over-sea distances.

Next, we studied directionality (anisotropy) in synchrony. This part of the analysis had two steps. First, to estimate the overall directionality of synchrony using the `Sncf2D` function in the `ncf` library to estimate the anisotropic correlation function at 22.5-degree intervals (16 compass directions) around the compass, based on all years in the larval time series (Bjørnstad *et al.* 2002). Second, to relate the directionality in synchrony to inter-annual variation in spring wind directions, we grouped the larval time series into years with circular mean wind directions along the east-west axis or north-south axis. Subsequently, we estimated the anisotropic correlation functions again for these two groups of years separately. The logic of this analysis was that population growth rates in year t [$r_t = \log_e(N_t/N_{t-1})$] could be synchronized if spring winds in that year acted to distribute larvae among populations and thereby homogenizing N_t. For both parts of this analysis, our measure of the strength of synchrony in a given direction was the distance at which the correlation function fell to the average regional correlation.

Finally, we investigated the presence of travelling waves. To do this, we used the `Sncf2D` function to estimate the time-lagged anisotropic correlation function (Bjørnstad *et al.* 2002) based on the matrix of inter-site correlations between growth rates in year t and t-1. In the presence of a travelling wave, this

lagged correlation function should reach its maximum at a distance equal to the wave speed in the direction of wave propagation.

Results

Population dynamics across the study region

Our 19-year time series covered two consecutive peaks in the population cycles of *E. autumnata* and *O. brumata*, the first occurring in the early to mid 2000s and the second in the early to mid 2010s (Fig. 1). Population densities during the first peak were generally low for both moth species, while both species reached densities high enough to inflict severe defoliation across most of the study region during the second peak. During the second peak, populations of *O. brumata* reached maximum densities 1-2 years later than *E. autumnata* at most sites, thus conforming to the typical pattern of phase-lagged dynamics when the two species occur in sympatry (Klemola *et al.* 2009). This pattern was less clear during the first peak, with substantial variation in the relative timing of peak densities for the two moth species across the study region.

Synchrony

As expected from the higher adult dispersal capacity of *E. autumnata*, spatial synchrony was considerably stronger in the population dynamics of *E. autumnata* than of *O. brumata*. The average regional correlation for *E. autumnata* was 0.56 [95 % bootstrap CI: 0.52, 0.60] while it was 0.35 [95 % bootstrap CI: 0.32, 0.38] for *O. brumata*. The synchrony declined with distance in both moth species, with a tendency for steeper decline at relatively short distances for *O. brumata*. Further, the difference between the two moth species was also evident in the effect of the open-sea dispersal barrier (Fig. 3). Here, the estimated drop in synchrony when moving across sea (an average distance of 5.7 kilometers) was -0.12 [95 % CI: -0.16, -0.08] for *E. autumnata*, while it was -0.31 [95 % CI: -0.35, -0.27] for *O. brumata*, consistent with a substantially stronger effect of the dispersal barrier in the latter species. Contrary to expectations, the linear mixed models of synchrony on distance within transects suggested that the drop in synchrony when moving across sea was less pronounced than what would be expected

from the drop in synchrony with distance when moving through continuous birch forest within transects (Fig. 3).

Anisotropic synchrony and wind direction

For the study period as a whole, spring winds displayed a predominantly east-west directionality. The overall circular mean direction for winds with a speed of more than 6 m/s was 269°, reflecting a predominance of wind directions in the range from 230° to 290° (Fig. 4A). This corresponds to winds coming from southwest to west-northwest. Winds coming from the opposite direction were also quite common, while winds along the north-south axis direction were comparatively rare. In accordance with this overall distribution, most individual years also displayed predominantly east-west wind directions (Fig. 4D). However, seven years (2003-2005, 2008, 2010, 2011 and 2017) had a circular mean wind direction indicating winds predominantly along the north-south axis. The direction of autumn winds showed a very similar distribution (Fig. S1), although in this case the predominance of west-southwest winds was even stronger than for spring winds.

In support of windborne larval dispersal as a potential synchronizing mechanism, the directionality of synchrony in moth population dynamics showed a clear congruence with the distribution of spring wind directions. Considering all years in the time series, the distance at which synchrony dropped to the regional average for both *E. autumnata* and *O. brumata* was in the range of 30-40 km (depending on the exact direction) along the east-west axis and 10-20 km along the north-south axis (Fig. 4B, C. See appendix table S1 for the exact distances at which synchrony fell to the regional average in each compass direction, including bootstrap confidence intervals). Thus, synchrony was most extensive parallel to the dominant wind direction. When years with predominantly east-west and north-south spring wind directions were considered separately, the directionality of synchrony remained strong for *E. autumnata* in east-west years, with the regional average synchrony being reached at distances of as far as 46 km along the east-west axis directions (Fig 4E). In conspicuous contrast to this, synchrony in *E. autumnata* was much weaker in years with predominantly north-south winds, falling to the regional average at distances below 15 km in all directions. Directional synchrony in *O. brumata* did not exhibit this

temporal structuring (Fig. 4F), and displayed a pattern that was relatively similar to the overall directionality of synchrony (Fig. 4C) in years dominated by both east-west and north-south winds.

Travelling waves

When moving from the east towards the southwest, the 1-year lagged anisotropic correlation functions for *E. autumnata* generally reached their peak at the maximum distance allowed by the dataset, i.e. 50-80 km depending on the direction (Fig. 5). The peak correlations were strongest in the southward direction (180°), reaching magnitudes of around 0.60 (see appendix table S2 for exact distances and correlations in each compass direction, including bootstrap confidence intervals). Meanwhile, the time-lagged correlation functions for *E. autumnata* indicated only weak lagged correlations (<0.26) for the northern half of the compass. This is compatible with a travelling wave moving roughly southwards at a speed of 50-80 km/year for *E. autumnata*. However, as the lagged correlations peaked at the maximum distances allowed by the dataset in the direction of wave propagation, it is theoretically possible that the correlations would have reached their true maxima at some unknown greater distance. Our estimate of the wave speed for *E. autumnata* is thus a minimum figure. For *O. brumata*, the lagged correlation functions were weak (<0.28) in all directions, providing no clear indications of travelling waves (Fig. 5).

Discussion

The role of dispersal in producing spatial patterns of synchrony in population dynamics has been the subject of numerous theoretical studies (Lande *et al.* 1999; Kendall *et al.* 2000; Engen, Lande & Sæther 2002; Goldwyn & Hastings 2008; Abbott 2011; Engen & Sæther 2016) and laboratory experiments (Fontaine & Gonzalez 2005; Vasseur & Fox 2009; Vogwill, Fenton & Brockhurst 2009; Fox *et al.* 2011; Howeth & Leibold 2013; Duncan, Gonzalez & Kaltz 2015). Meanwhile, work on dispersal-driven synchrony in the field has lagged behind, even for species where synchrony has received considerable attention, including *E. autumnata* and *O. brumata* (Ims *et al.* 2004; Klemola, Huitu & Ruohomaki 2006; Tenow *et al.* 2007; Hagen *et al.* 2008). Our current results advance the understanding of dispersal-driven

synchrony in natural populations, by showing that dispersal processes can leave clear signatures in both the strength and directionality of synchrony in carefully designed, field-collected time series.

The relationship between dispersal capacity and the strength of synchrony is evident from our comparison between *E. autumnata* and *O. brumata*. *O. brumata*, with flightless females, displayed overall a consistently weaker synchrony than *E. autumnata*, and the drop in synchrony induced by the open-sea dispersal barrier was much more pronounced in *O. brumata* than *E. autumnata*. Given the otherwise very similar ecology of the two moth species, it seems reasonable to attribute these patterns to the lower dispersal capacity during the adult stage of *O. brumata* (smaller adults with wingless females) than *E. autumnata* (larger adults with both sexes winged). This argues for adult dispersal as an important synchronizing mechanism at the spatial scale of the study. Because the two moth species were sampled at the exact same time and place, we can rule out context-dependencies in space or time as alternative explanations for the interspecific differences in synchrony. Species-specific biases related to the common sampling method also seem unlikely. Thus, the main potential caveat to a dispersal-based interpretation of the synchrony patterns is the presence of differential sensitivities to unknown environmental factors in the two moth species. If *O. brumata* and *E. autumnata* respond to different external synchronizing factors (e.g. weather parameters with different spatial autocorrelation), this could account for the consistently weaker synchrony in *O. brumata*. This alternative explanation cannot be ruled out at present and should be regarded as a competing hypothesis to synchronizing adult dispersal.

While the relative effects of the open-sea dispersal barrier on *E. autumnata* and *O. brumata* are easily interpreted in terms of the lower dispersal capacity of *O. brumata*, the absolute effect of the barrier on dispersal and synchrony in either moth species is difficult to infer. Ideally, synchrony should have been compared between the barrier and a control stretch of core habitat (i.e. continuous birch forest) of similar length (Roland & Matter 2007), which was not feasible due to logistic and topographical constraints. When the linear drop in synchrony within transects was extrapolated to over-sea distances, the predicted synchrony declined more rapidly than what was actually observed over sea. A possible explanation for this is that within-transect synchrony is mainly driven by short-distance dispersal, which declines rapidly

with distance, while synchrony across longer distances is dominated by long-distance dispersal and the Moran effect, which may cause synchrony to decay with distance at a very different rate. Thus, the local decline in synchrony within transects probably represents an inadequate null model for longer distances. Further, although open sea is a hostile habitat, higher wind speeds and fewer obstructions could potentially cause windborne dispersal over sea to be more efficient than over land, similarly to what has been found for plant seeds dispersing through open versus forested habitats (Roberts *et al*. 2018). Thus, the effect of sea as a dispersal barrier may not be as straightforward as one would first think.

Showing that synchrony is stronger in more dispersive species is perhaps the most common evidence for dispersal-driven synchrony in field populations (Koenig 1998; Paradis *et al*. 1999; Chevalier, Laffaille & Grenouillet 2014). In the current study, we have also implemented a more sophisticated approach by relating the directionality of synchrony to dispersal-related wind data. Considering the study period as a whole, there was remarkably good congruence between the dominant wind direction during the larval dispersal period and the direction that showed the most spatially extensive synchrony in both *E. autumnata* and *O. brumata*. These patterns are most easily explained by increased rate and/or scale of windborne larval dispersal in the predominant wind direction. Notably, wind directions during autumn were very similar to those of spring, and thereby also congruent with the direction of highest synchrony in both moth species. Thus, windborne adult dispersal may have contributed to the directionality of synchrony in *E. autumnata*, whose adult females can fly. However, the fact that synchrony aligned with wind direction also for *O. brumata*, whose females are flightless, suggests that windborne larval dispersal alone is enough to determine the directionality of synchrony.

The results were less conclusive when years with predominantly east-west and north-south winds were considered separately. Years dominated by north-south winds saw almost complete disappearance of synchrony in *E. autumnata*, but maintenance of a clear east-west structuring of synchrony in *O. brumata*. When interpreting these patterns, it should be remembered that only seven years in our time series had predominantly north-south winds. Moreover, many of these years had low-density moth populations (Fig. 1), where our density measure usually contains many zeroes and sampling variation is high. Thus,

390 the anisotropic analysis for these years carries higher uncertainty. However, it is not implausible that
391 anisotropic synchrony structured mainly along the east-west axis breaks down in years dominated by
392 north-south winds, as the results for *E. autumnata* suggest. At the same time, it is also conceivable that
393 such years would not disrupt a strong east-west synchrony induced by long-term predominance of east-
394 west winds, as suggested by the results for *O. brumata*. Given the divergent results for the two moth
395 species, we cannot presently conclude on this point, and longer time series or theoretical modelling
396 studies may be needed to resolve the issue.
397
398 Although dispersal in many insect species is influenced by wind to some extent (Gatehouse 1997;
399 Compton 2002), the relationship between wind patterns and spatial synchrony in insects has thus far
400 received surprisingly little attention. A notable exception is the study of Bearup *et al.* (2013), which
401 supported wind-driven dispersal as a driver of directional synchrony in populations of the crane fly
402 *Tipula paludosa* (Meigen) in agricultural fields in Scotland. This aligns with the present study and
403 highlights wind-driven dispersal as a mechanism that deserves more attention in studies of spatial
404 synchrony in insects. Our current results show that this topic can be explored using relatively simple
405 methods, but more sophisticated approaches could provide even stronger inference about wind-driven
406 synchrony. For example, higher resolution wind models could be coupled with models of particle spread
407 (Lander *et al.* 2014) to predict detailed dispersal patterns and thus help formulate more precise
408 predictions about the directionality of synchrony.
409
410 Overall, our results support both adult and larval dispersal as important synchronizing factors for meso-
411 scale population dynamics in the focal geometrid species. A corollary of this is that gene flow between
412 local geometrid populations should be substantial at this scale. This prediction can be tested using
413 spatially targeted genetic studies. In the presence of high gene flow rates, we predict that moth
414 populations within the current study region will show minimal spatial genetic structuring, and that the
415 sampling frame must be expanded to uncover the scale at which genetic structure becomes apparent.
416 Leggett *et al.* (2011) demonstrated low levels of genetic differentiation among *O. brumata* populations
417 across a study region of comparable spatial extent to the present study in the Orkney islands, and

418 suggested that this was due to high gene flow resulting from dispersal of ballooning larvae. Genetic
419 evidence for high rates of gene flow and dispersal across distances of tens to hundreds of kilometers has
420 recently also been obtained for two other cyclic lepidopteran defoliators: the western tent caterpillar
421 (*Malacosoma californicum pluviale* Packard) (Franklin, Myers & Cory 2014) and the eastern spruce
422 budworm (*Choristoneura fumiferana* Clemens) (James *et al.* 2015). In both cases, the authors suggested
423 that dispersal plays an important role in synchronizing populations at the spatial scales considered.
424
425 The presence of directional dependencies in synchrony was also evident in the lagged correlation
426 functions for *E. autumnata*. For this species, we detected strong 1-year lagged correlations at distances
427 of 50-80 km when moving roughly southwards, suggesting the presence of a travelling wave moving in
428 this direction. This is in good accordance with the east-west directionality of within-year synchrony, as
429 within-year synchrony (and dispersal) is expected to be more extensive parallel to the front of a
430 travelling wave than in the direction of wave propagation (Berthier *et al.* 2014). Although the concept
431 of travelling waves has been much discussed for geometrid moths (Tenow *et al.* 2007; Tenow *et al.*
432 2013; Jepsen *et al.* 2016; Tenow 2016), this is the first formal statistical analysis to provide evidence of
433 waves based on quantitative time series for these species. Nevertheless, caution is needed when
434 interpreting the evidence for a wave in *E. autumnata*. First, the lagged anisotropic correlation functions
435 reached their peak at the maximum distance provided by the dataset in the direction of wave propagation.
436 The true maxima of these functions may therefore occur at even greater distances. This may well be the
437 case, as the strongest lagged correlation in our data (0.61) was only slightly stronger than the regional
438 average (0.56) of the within-year correlations; an observation that would be consistent with unobserved
439 greater maxima for the lagged correlations (although with the caveat that the strength of within-year and
440 lagged correlations may not be directly comparable). The presence of unobserved maxima for the lagged
441 correlations would cause our estimated wave speed of 50-80 km/year to be downward biased, and we
442 therefore stress that this estimate represents a minimum figure. A second issue concerns the direction of
443 the wave. Reaction-diffusion models show that waves can radiate from areas of unsuitable habitat (i.e.
444 hostile boundaries) (Sherratt & Smith 2008). In our case, the open ocean is an obvious hostile boundary,
445 and borders our study region to both the north and west. A southward wave is consistent with the

northern coast as a hostile boundary, but is harder to reconcile with the western coast. However, it is difficult to predict how a wave will behave in a region bordered by multiple hostile boundaries, and sampling with higher spatial resolution may be needed to detect subtler spatial dynamics that could arise in this situation. Finally, there was no evidence for waves in *O. brumata*. Since *O. brumata* is a cyclic oscillator that is very similar to *E. autumnata*, it is unclear why only one of the species should exhibit waves in a system where the two occur in sympatry and both exhibit cycles. Thus, although our current results are compatible with a wave in *E. autumnata*, further work is required to confirm that waves are an important feature of meso-scale geometrid dynamics.

Our study adds new perspectives to the conclusions of Ims *et al.* (2004), who presented the first four years of our *O. brumata* time series. Their main conclusion was that *O. brumata* populations in coastal birch forest could be spatially asynchronous over short distances, based on the finding that some neighboring populations appeared to be in different phases of the population cycle (peak vs. through) during 1999-2002. The first half of our time series, including the years studied by Ims *et al*. (2004), confirm that there can be substantial spatial heterogeneity in the timing of *O. brumata* population peaks in our study region (Fig. 1). However, the second half of the time series presents considerably lower variance in the timing of peaks, showing that these populations can also conform to the regional synchrony that has traditionally been assumed to be the rule for cyclic geometrids in Scandinavia (Tenow 1972). It is thus evident that spatial synchrony in *O. brumata* in our system may vary between different realizations of the population cycle, perhaps reflecting variation in the action of synchronizing environmental factors or unknown conditions affecting dispersal rates.

Conclusions

Our results indicate that larval and adult dispersal leave detectable signatures in the strength and directionality, respectively, of meso-scale spatial synchrony in the focal pair of geometrid defoliators. This aligns with accumulating evidence for dispersal as an important synchronizing mechanism across distances of tens to hundreds of kilometers in cyclic lepidopterans, and highlights wind-driven dispersal as a particularly promising avenue of investigation to deepen the understanding of spatial synchrony in

winged or ballooning natural insect populations. Studies of gene flow in *E. autumnata* and *O. brumata* now represent the next logical step of investigation to substantiate the present evidence for dispersal as an important driver of meso-scale synchrony in these species.

Acknowledgements

Our ongoing monitoring of geometrid population dynamics has benefitted from the fieldwork of many researchers, students and field assistants over the years. Although we cannot mention all of their names, thanks are due to everyone who has contributed. We would like to give special mention to Snorre B. Hagen, Tino Schott, Lauri Kapari and Malin Ek for their invaluable contributions. The monitoring has received financial support from the Norwegian Research Council (grants 171026/V40, 144885/E10, 244454/E10), the Norwegian Institute for Nature Research and the Institute of Arctic and Marine Biology, University of Tromsø. Finally, we are grateful to two anonymous reviewers, who provided constructive comments on the manuscript.

Data accessibility

Data deposited in the Dryad repository: http://datadryad.org/resource/doi:10.5061/dryad.kb4867v (Vindstad *et al.* 2019).

References

Abbott, K.C. (2011) A dispersal-induced paradox: synchrony and stability in stochastic metapopulations. *Ecology Letters*, **14,** 1158-1169.

Anderson, T.L., Walter, J.A., Levine, T.D., Hendricks, S.P., Johnston , K.L., White, D.S. & Reuman, D.C. (2018) Using geography to infer the importance of dispersal for the synchrony of freshwater plankton. *Oikos*, **127,** 403-414.

Bearup, D., Petrovskii, S., Blackshaw, R. & Hastings, A. (2013) Synchronized Dynamics of *Tipula paludosa* Metapopulation in a Southwestern Scotland Agroecosystem: Linking Pattern to Process. *The American Naturalist*, **182,** 393-409.

Berthier, K., Piry, S., Cosson, J.-F., Giraudoux, P., Foltête, J.-C., Defaut, R., Truchetet, D. & Lambin, X. (2014) Dispersal, landscape and travelling waves in cyclic vole populations. *Ecology Letters,* **17,** 53-64.

Bjørnstad, O.N. & Falck, W. (2001) Nonparametric spatial covariance functions: Estimation and testing. *Environmental and Ecological Statistics,* **8,** 53-70.

Bjørnstad, O.N., Ims, R.A. & Lambin, X. (1999) Spatial population dynamics: analyzing patterns and processes of population synchrony. *Trends in Ecology & Evolution,* **14,** 427-432.

Bjørnstad, O.N., Peltonen, M., Liebhold, A.M. & Baltensweiler, W. (2002) Waves of Larch Budmoth Outbreaks in the European Alps. *Science,* **298,** 1020-1023.

Bylund, H. (1999) Climate and the population dynamics of two insect outbreak species in the north. *Ecological Bulletins,* **47,** 54-62.

Chevalier, M., Laffaille, P. & Grenouillet, G. (2014) Spatial synchrony in stream fish populations: influence of species traits. *Ecography,* **37,** 960-968.

Compton, S.G. (2002) Sailing with the wind: dispersal by small flying insects. *Dispersal Ecology: 42nd Symposium of the British Ecological Society* (eds J.M. Bullock, R.E. Kenward & R.S. Hails), pp. 113-133. Cambridge University Press.

Dee, D.P., Uppala, S.M., Simmons, A.J., Berrisford, P., Poli, P., Kobayashi, S., Andrae, U., Balmaseda, M.A., Balsamo, G., Bauer, P., Bechtold, P., Beljaars, A.C.M., van de Berg, L., Bidlot, J., Bormann, N., Delsol, C., Dragani, R., Fuentes, M., Geer, A.J., Haimberger, L., Healy, S.B., Hersbach, H., Hólm, E.V., Isaksen, L., Kållberg, P., Köhler, M., Matricardi, M., McNally, A.P., Monge-Sanz, B.M., Morcrette, J.-J., Park, B.K., Peubey, C., de Rosnay, P., Tavolato, C., Thépaut, J.N. & Vitart, F. (2011) The ERA-Interim reanalysis: configuration and performance of the data assimilation system. *Quarterly Journal of the Royal Meteorological Society,* **137,** 553-597.

Duncan, A.B., Gonzalez, A. & Kaltz, O. (2015) Dispersal, environmental forcing, and parasites combine to affect metapopulation synchrony and stability. *Ecology,* **96,** 284-290.

Edland, T. (1971) Wind dispersal of the winter moth *Operophtera brumata* L. (Lep., Geometridae) and its relevance to control measures. *Norsk Entomologisk Tidskrift,* **18,** 103-105.

529 Engen, S., Lande, R. & Sæther, B.-E. (2002) Migration and spatiotemporal variation in population
530 dynamics in a heterogeneous environment. *Ecology,* **83,** 570-579.
531 Engen, S. & Sæther, B.-E. (2016) Spatial synchrony in population dynamics: The effects of
532 demographic stochasticity and density regulation with a spatial scale. *Mathematical*
533 *Biosciences,* **274,** 17-24.
534 Fontaine, C. & Gonzalez, A. (2005) Population synchrony induced by resource fluctuations and
535 dispersal in an aquatic microcosm. *Ecology,* **86,** 1463-1471.
536 Fox, J.W., Vasseur, D.A., Hausch, S. & Roberts, J. (2011) Phase locking, the Moran effect and
537 distance decay of synchrony: experimental tests in a model system. *Ecology Letters,* **14,** 163-
538 168.
539 Franklin, M.T., Myers, J.H. & Cory, J.S. (2014) Genetic Similarity of Island Populations of Tent
540 Caterpillars during Successive Outbreaks. *Plos One,* **9,** e96679.
541 Gatehouse, A.G. (1997) Behavior and ecological genetics of wind-borne migration by insects. *Annual*
542 *Review of Entomology,* **42,** 475-502.
543 Goldwyn, E.E. & Hastings, A. (2008) When can dispersal synchronize populations? *Theoretical*
544 *Population Biology,* **73,** 395-402.
545 Gouveia, A.R., Bjørnstad, O.N. & Tkadlec, E. (2016) Dissecting geographic variation in population
546 synchrony using the common vole in central Europe as a test bed. *Ecology and Evolution,* **6,**
547 212-218.
548 Grenfell, B.T., Wilson, K., Finkenstädt, B.F., Coulson, T.N., Murray, S., Albon, S.D., Pemberton,
549 J.M., Clutton-Brock, T.H. & Crawley, M.J. (1998) Noise and determinism in synchronized
550 sheep dynamics. *Nature,* **394,** 674.
551 Hagen, S.B., Jepsen, J.U., Yoccoz, N.G. & Ims, R.A. (2008) Anisotropic patterned population
552 synchrony in climatic gradients indicates nonlinear climatic forcing. *Proceedings of the Royal*
553 *Society B-Biological Sciences,* **275,** 1509-1515.
554 Haynes, K.J., Bjørnstad, O.N., Allstadt, A.J. & Liebhold, A.M. (2013) Geographical variation in the
555 spatial synchrony of a forest-defoliating insect: isolation of environmental and spatial drivers.
556 *Proceedings of the Royal Society of London B: Biological Sciences,* **280**.

Howeth, J.G. & Leibold, M.A. (2013) Predation inhibits the positive effect of dispersal on intraspecific and interspecific synchrony in pond metacommunities. *Ecology,* **94,** 2220-2228.

Ims, R.A. & Andreassen, H.P. (2000) Spatial synchronization of vole population dynamics by predatory birds. *Nature,* **408,** 194-196.

Ims, R.A. & Andreassen, H.P. (2005) Density-Dependent Dispersal and Spatial Population Dynamics. *Proceedings of the Royal Society B - Biological Sciences,* **272,** 913-918.

Ims, R.A., Yoccoz, N.G. & Hagen, S.B. (2004) Do sub-Arctic winter moth populations in coastal birch forest exhibit spatially synchronous dynamics? *Journal of Animal Ecology,* **73,** 1129-1136.

James, P.M.A., Cooke, B., Brunet, B.M.T., Lumley, L.M., Sperling, F.A.H., Fortin, M.-J., Quinn, V.S. & Sturtevant, B.R. (2015) Life-stage differences in spatial genetic structure in an irruptive forest insect: implications for dispersal and spatial synchrony. *Molecular Ecology,* **24,** 296-309.

Jammalamadaka, S.R. & Sengupta, A. (2001) *Topics in Circular Statistics*. World Scientific.

Jepsen, J.U., Hagen, S.B., Karlsen, S.R. & Ims, R.A. (2009) Phase-dependent outbreak dynamics of geometrid moth linked to host plant phenology. *Proceedings of the Royal Society B-Biological Sciences,* **276,** 4119-4128.

Jepsen, J.U., Vindstad, O.P.L., Barraquand, F., Ims, R.A. & Yoccoz, N.G. (2016) Continental-scale travelling waves in forest geometrids in Europe: an evaluation of the evidence. *Journal of Animal Ecology,* **85,** 385-390.

Karlsen, S.R., Solheim, I., Beck, P.S.A., Høgda, K.A., Wielgolaski, F.E. & Tømmervik, H. (2007) Variability of the start of the growing season in Fennoscandia, 1982-2002. *International Journal of Biometeorology,* **51,** 513-524.

Kendall, B.E., Bjørnstad, O.N., Bascompte, J., Keitt, T.H. & Fagan, W.F. (2000) Dispersal, Environmental Correlation, and Spatial Synchrony in Population Dynamics. *The American Naturalist,* **155,** 628-636.

583 Klemola, N., Heisswolf, A., Ammunet, T., Ruohomäki, K. & Klemola, T. (2009) Reversed impacts by
584 specialist parasitoids and generalist predators may explain a phase lag in moth cycles: a novel
585 hypothesis and preliminary field tests. *Annales Zoologici Fennici,* **46,** 380-393.
586 Klemola, T., Huitu, O. & Ruohomäki, K. (2006) Geographically partitioned spatial synchrony among
587 cyclic moth populations. *Oikos,* **114,** 349-359.
588 Koenig, W.D. (1998) Spatial Autocorrelation in California Land Birds. *Conservation Biology,* **12,**
589 612-620.
590 Lande, R., Engen, S. & Sæther, B.-E (1999) Spatial Scale of Population Synchrony: Environmental
591 Correlation versus Dispersal and Density Regulation. *The American Naturalist,* **154,** 271-281.
592 Lander, T.A., Klein, E.K., Oddou-Muratorio, S., Candau, J.-N., Gidoin, C., Chalon, A., Roig, A.,
593 Fallour, D., Auger-Rozenberg, M.-A. & Boivin, T. (2014) Reconstruction of a windborne
594 insect invasion using a particle dispersal model, historical wind data, and Bayesian analysis of
595 genetic data. *Ecology and Evolution,* **4,** 4609-4625.
596 Leggett, H.C., Jones, E.O., Burke, T., Hails, R.S., Sait, S.M. & Boots, M. (2011) Population genetic
597 structure of the winter moth, *Operophtera brumata* Linnaeus, in the Orkney Isles suggests
598 long-distance dispersal. *Ecological Entomology,* **36,** 318-325.
599 Liebhold, A., Koenig, W.D. & Bjørnstad, O.N. (2004) Spatial Synchrony in Population Dynamics.
600 *Annual Review of Ecology, Evolution, and Systematics,* **35,** 467-490.
601 Mesquita, M.d.S., Erikstad, K.E., Sandvik, H., Barrett, R.T., Reiertsen, T.K., Anker-Nilssen, T.,
602 Hodges, K.I. & Bader, J. (2015) There is more to climate than the North Atlantic Oscillation: a
603 new perspective from climate dynamics to explain the variability in population growth rates of
604 a long-lived seabird. *Frontiers in Ecology and Evolution,* **3**.
605 Mjaaseth, R.R., Hagen, S.B., Yoccoz, N.G. & Ims, R.A. (2005) Phenology and abundance in relation
606 to climatic variation in a sub-arctic insect herbivore-mountain birch system. *Oecologia,* **145,**
607 53-65.
608 Moss, R., Elston, D.A. & Watson, A. (2000) Spatial Asynchrony and Demographic Traveling Waves
609 during Red Grouse Population Cycles. *Ecology,* **81,** 981-989.

610 Myers, J.H. & Cory, J.S. (2013) Population Cycles in Forest Lepidoptera Revisited. *Annual Review of*
611 *Ecology, Evolution, and Systematics*, **44,** 565-592.
612 Paradis, E., Baillie, S.R., Sutherland, W.J. & Gregory, R.D. (1999) Dispersal and spatial scale affect
613 synchrony in spatial population dynamics. *Ecology Letters*, **2,** 114-120.
614 Peltonen, M., Liebhold, A.M., Bjørnstad, O.N. & Williams, D.W. (2002) Spatial Synchrony in Forest
615 Insect Outbreaks: Roles of Regional Stochasticity and Dispersal. *Ecology*, **83,** 3120-3129.
616 Post, E. & Forchhammer, M.C. (2002) Synchronization of animal population dynamics by large-scale
617 climate. *Nature*, **420,** 168-171.
618 R Developement Core Team (2017) R: A language and environment for statistical conputing. R
619 foundation for statistical computing, Vienna, Austria.
620 Roberts, D., Ciuti, S., Barber, Q.E., Willier, C. & Nielsen, S.E. (2018) Accelerated seed dispersal
621 along linear disturbances in the Canadian oil sands region. *Scientific reports*, **8**, 4828-4828.
622 Roland, J. & Matter, S.F. (2007) Encroaching forests decouple alpine butterfly population dynamics.
623 *Proceedings of the National Academy of Sciences*, **104,** 13702-13704.
624 Sandhya, S. (2012) A meta-analysis of the traits affecting dispersal ability in butterflies: can wingspan
625 be used as a proxy? *Journal of Animal Ecology*, **81,** 174-184.
626 Sherratt, J.A. & Smith, M.J. (2008) Periodic travelling waves in cyclic populations: field studies and
627 reaction–diffusion models. *Journal of The Royal Society Interface*, **5,** 483-505.
628 Snäll, N., Huoponen, K., Saloniemi, I., Savontaus, M.-L. & Ruohomäki, K. (2004) Dispersal of
629 females and differentiation between populations of *Epirrita autumnata* (Lepidoptera:
630 Geometridae) inferred from variation in mitochondrial DNA. *Europeean Journal of*
631 *Entomology*, **101**, 495-502.
632 Straussfogel, D., Lindgren, B.S., Mitchell, S., Murphy, B. & Jackson, P.L. (2008) Radar observation
633 and aerial capture of mountain pine beetle, *Dendroctonus ponderosae* Hopk. (Coleoptera:
634 Scolytidae) in flight above the forest canopy. *Canadian Journal of Forest Research*, **38,** 2313-
635 2327.

636 Tenow, O. (1972) The outbreaks of *Oporinia autumnata* Bkh. and *Operophtera* spp. (Lep.,
637 Geometridae) in the Scandinavian mountain chain and northern Finland 1862-1968.
638 Zoologiska bidrag från Uppsala, Supplement, 2, 1-107.
639 Tenow, O. (2016) A response to Jepsen et al. (2016). *Journal of Animal Ecology,* **85,** 391-395.
640 Tenow, O., Nilssen, A.C., Bylund, H. & Hogstad, O. (2007) Waves and synchrony in *Epirrita*
641 *autumnata/Operophtera brumata* outbreaks. I. Lagged synchrony: regionally, locally and
642 among species. *Journal of Animal Ecology,* **76,** 258-268.
643 Tenow, O., Nilssen, A.C., Bylund, H., Pettersson, R., Battisti, A., Bohn, U., Caroulle, F., Ciornei, C.,
644 Csóka, G., Delb, H., De Prins, W., Glavendekić, M., Gninenko, Y.I., Hrašovec, B., Matošević,
645 D., Meshkova, V., Moraal, L., Netoiu, C., Pajares, J., Rubtsov, V., Tomescu, R. & Utkina, I.
646 (2013) Geometrid outbreak waves travel across Europe. *Journal of Animal Ecology,* **82,** 84-
647 95.
648 Vasseur, D.A. & Fox, J.W. (2009) Phase-locking and environmental fluctuations generate synchrony
649 in a predator–prey community. *Nature,* **460,** 1007-1010.
650 Vindstad, O.P.L., Jepsen, J.U., Yoccoz, N.G., Bjørnstad, O.N., Mesquita, M.d.S. & Ims, R.A. (2019)
651 Data from: Spatial synchrony in sub-arctic geometrid moth outbreaks reflects dispersal in
652 larval and adult lifecycle stages. *Journal of Animal Ecology*, doi: 10.5061/dryad.kb4867v.
653 Vogwill, T., Fenton, A. & Brockhurst, M.A. (2009) Dispersal and natural enemies interact to drive
654 spatial synchrony and decrease stability in patchy populations. *Ecology Letters,* **12,** 1194-
655 1200.

656
657
658
659
660
661
662

Figures

Figure 1.

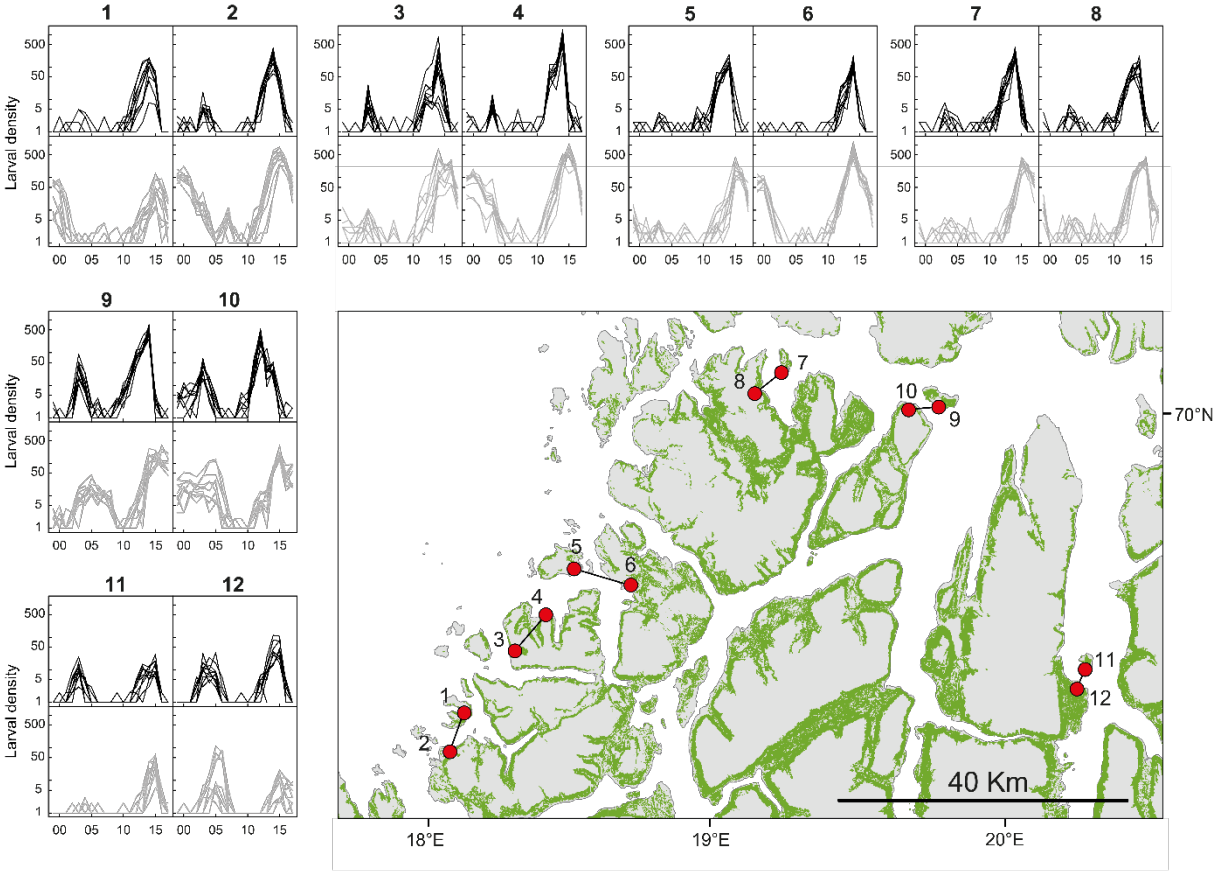

678 Figure 2.

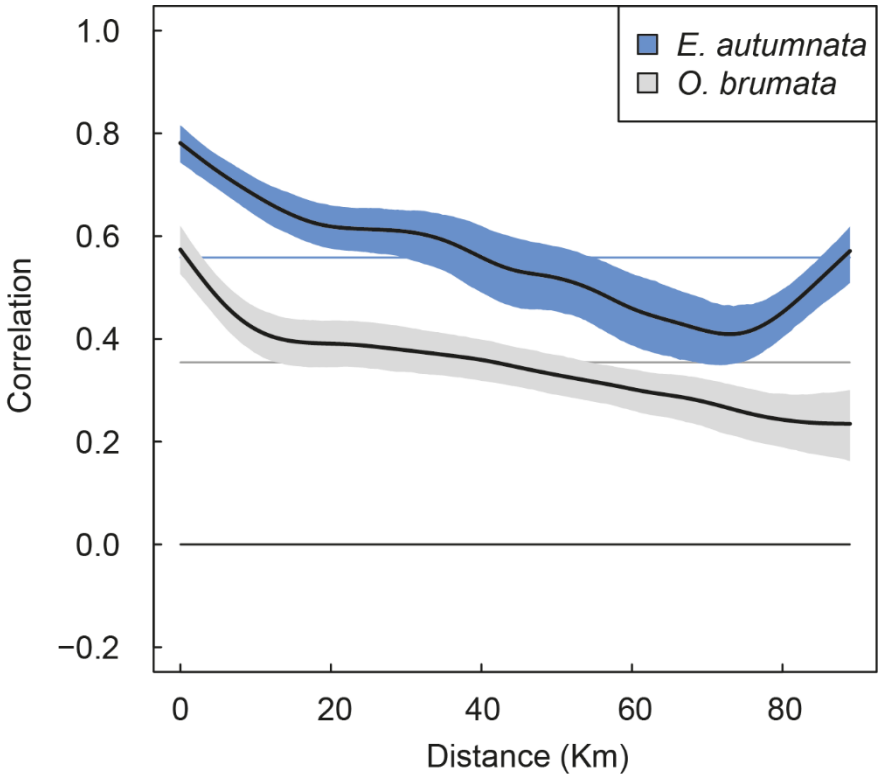

679

680

681 Figure 3.

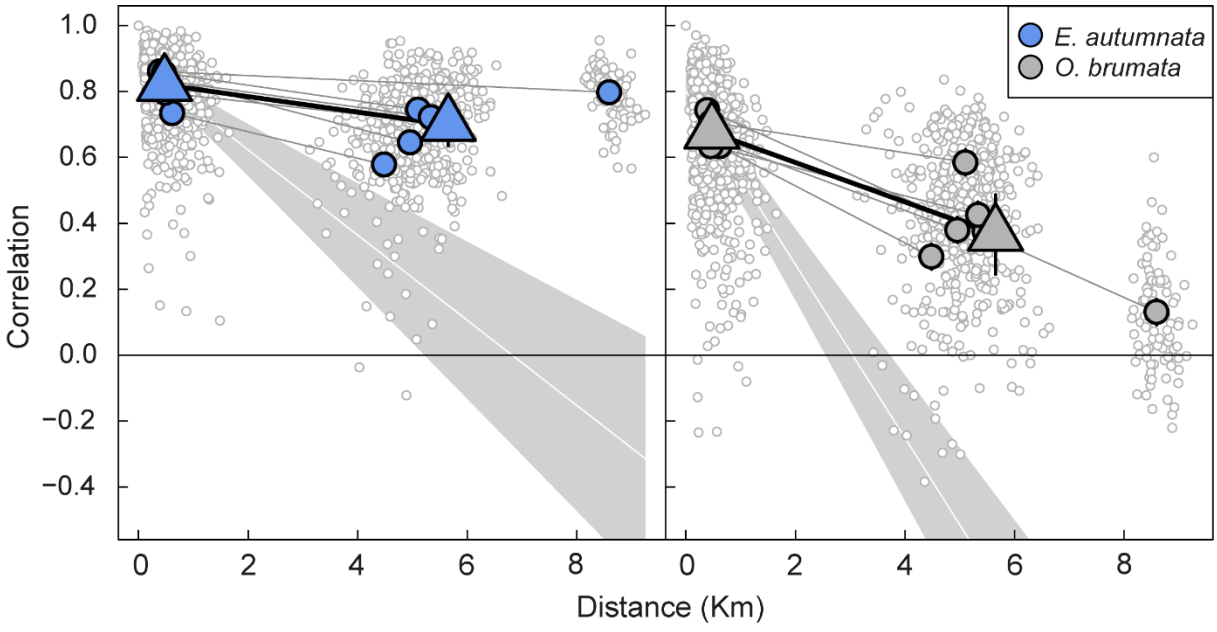

682

683

684

685

Figure 4.

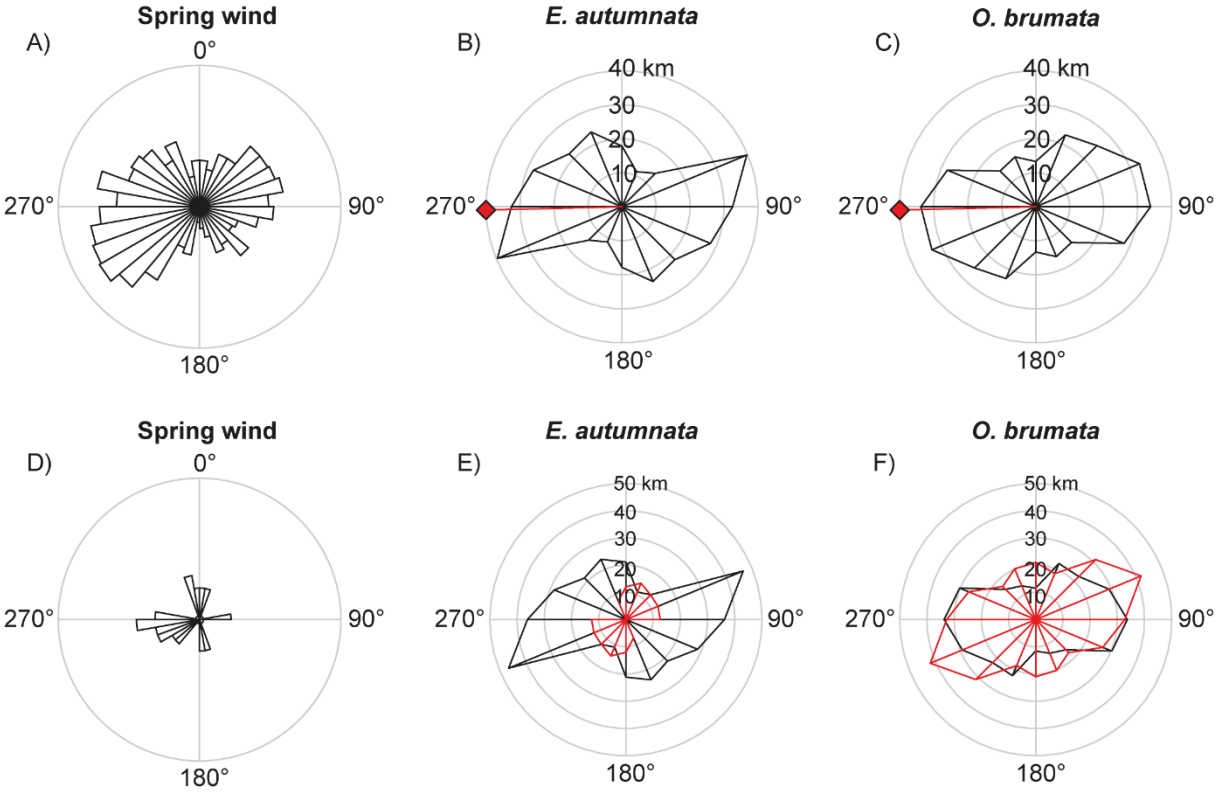

Figure 5.

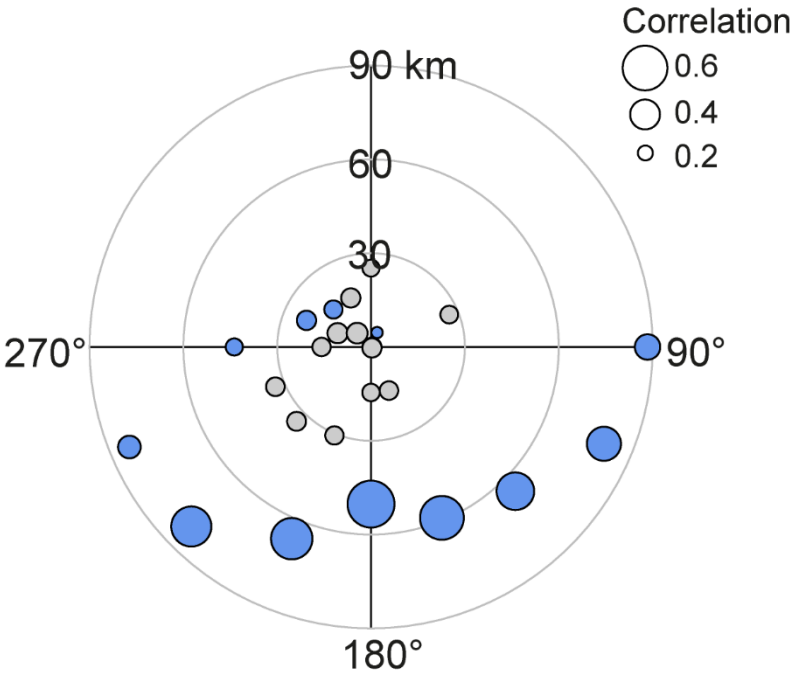

Figure legends

692 Figure 1. Map of the study region with time series of *E. autumnata* (black lines) and *O. brumata* (grey
693 lines) larvae for 1999-2017 from each of the twelve sampling transects (red dots in the map). Transects
694 belonging to the same island-continent pair are joined by a line. Green areas in the map represent
695 mountain birch forest. Individual lines in the time series plots represent the series from each of the ten
696 sampling stites within each transect. Larval density is the sum of larvae across ten birch branches. The
697 X axis is the number of years after 2000.
698
699 Figure 2. Isotropic nonparametric correlation functions showing the decline in synchrony with distance
700 across the study region for *E. autumnata* and *O. brumata*. Bold solid lines represent the estimated
701 correlation function while the shaded areas represent 95 % bootstrap confidence intervals. The
702 correlation functions were estimated with 6 degrees of freedom. Horizontal lines represent the mean
703 correlation across the study region (i.e. the regional synchrony) for each moth species.
704
705 Figure 3. Correlations in population growth rates between sites within island-continent pairs (small dots)
706 plotted against distance for *E. autumnata* and *O. brumata*. The cloud of points below two-km distances
707 represent correlations within transects. Remaining points are correlations between transects (i.e. across
708 sea). Large symbols represent estimated effects from linear mixed models taking the correlations as the
709 response variable, and the within transect vs. between transect contrast as a categorical predictor. Large
710 triangles represent fixed effects from the models, while large circles represent random effects for the six
711 island-continent pairs. The random effects are plotted at the mean distances for their respective transects,
712 while the fixed effects are plotted at the overall mean distances. Error bars represent 95 % confidence
713 intervals (in most cases smaller than the symbols) for the estimated effects. The white lines represent
714 predictions from linear mixed models of synchrony on distance, that have been fitted to the data points
715 within transects and extrapolated to over-sea distances. Shaded areas represent 95 % confidence
716 intervals for the predictions.
717
718 Figure 4. A) Rose diagram showing the distribution of wind directions (6-hour intervals) across the
719 study region for the period of potential larval dispersal (1. May – 15. June) across 1999 – 2017. The

length of the bars is proportional to the frequency of observations in 10° bins. B and C) Circular diagrams for anisotropic nonparametric correlation functions for *E. autumnata* (B) and *O. brumata* (C), based on the entire larval time series (1999-2017). The edge of the polygons represents the distance (in km) at which the correlation function falls to the regional average correlation in each of 16 directions (22.5° intervals). The red diamonds represents the circular mean of the wind directions summarized in panel A. D) Rose diagram showing the distribution of annual mean wind directions for the period of larval dispersal (1. May – 15. June) across 1999 – 2017. E and F) Circular diagrams for anisotropic nonparametric correlation functions for *E. autumnata* (E) and *O. brumata* (F), based on years with a mean east-west wind direction (black polygons) and a mean north-south wind direction (red polygons). The edge of the polygons represent the distance (in km) at which the correlation function falls to the regional average correlation in each of 16 directions (22.5° intervals). For directions where the polygon has no edge, the correlation is equal to (or lower than) the regional average already at a distance of zero km. Zero degrees represents north in all panels. Ninety-five % bootstrap confidence intervals for panels B, C, E and F are provided in table S1 of the appendix.

Figure 5. Circular diagram for 1-year-lagged anisotropic nonparametric correlation functions for *E. autumnata* (blue circles) and *O. brumata* (grey circles), based on the larval time series for 1999-2017. The distances of the circles from the origin represent the distance (in km) where the lagged correlation function reaches its maximum in each of 16 directions (22.5° intervals). The size of the circles is proportional to the correlation at the maximum of the function (see legend). Note that the correlation function reaches its maximum at a distance of zero km in several directions for both moth species. Table S2 in the appendix provides 95 % bootstrap confidence intervals for the distance of maximum correlation, and the magnitude of correlation at that distance, in each direction.